THERMAL SIMULATION: A BACKUP FOR BUILDING THERMOGRAPHY APPLICATIONS TO DETECT DELAMINATION

Ecem Edis[1]
[1] Istanbul Technical University - Faculty of Architecture, Istanbul, Turkey

ABSTRACT

Infrared thermography (IRT) is a non-destructive inspection method that is used to detect delamination in building elements. To detect delamination, dynamic thermal conditions are required, and therefore, determining proper inspection time becomes important, and thermogram interpretation becomes a complex process. To predict thermal response of building element inspected, thermal simulation can be used as a tool.

In the paper, following brief theoretical information on IRT and delamination detection, use of thermal simulation is exemplified for IRT inspection of buildings in Istanbul (Turkey) with exterior thermal insulation composite system (ETICS). Simulation results are then evaluated to discuss the potential of IRT in detecting delamination between ETICS layers.

INTRODUCTION

Infrared thermography (IRT) is a non-destructive method used for detecting building pathologies such as thermal irregularities, air infiltration, increased moisture, and delamination of a component from its substrate. To detect thermal irregularities and air infiltration, steady thermal conditions are usually preferred (ISO, 1983). Therefore, it is usually not necessary to predict thermal response of inspected element over time, unless defect characterisation is aimed. On the other hand, dynamic (thermal) conditions are usually needed to detect delamination and moisture increase (Chew, 1998; Edis et al, 2015; Rosina and Ludwig, 1999). However, in that case, it is necessary to predict (hygro)thermal response of the element inspected in order to determine proper inspection time and provide data for interpreting thermograms, where performance simulation can be benefited from.

In the paper, delamination detection by IRT and use of thermal simulation in this process is considered. Initially, theoretical information on IRT and its use in delamination detection is provided. Use of thermal simulation is then exemplified for the exterior IRT inspection of an exterior thermal insulation composite system (ETICS) in Istanbul (Turkey). Finally, simulation results are evaluated to discuss the potential of IRT in detecting delamination and to determine proper IRT inspection period.

THEORETICAL CONSIDERATIONS ON IRT AND DELAMINATION DETECTION

In IRT, a thermal image (thermogram) of the surface is formed considering infrared radiation emitted by and reflected from the surface. Surface temperature distribution is then evaluated to detect the anomalies.

In building thermography, natural (environmental) conditions or artificial heat sources can be used to trigger surface temperature variations. In the case of exterior inspection of middle to high-rise buildings, use of natural environmental conditions allows benefiting from the remote nature of the method.

In delamination detection by IRT, dynamic thermal conditions are preferred, since the additional thermal resistance provided by the air gap formed by the delamination is usually not sufficient to generate observable surface temperature variations under steady conditions (Santos et al, 2003). Under dynamic conditions, during the heating period, the air gap acts as insulator and surface temperature of the defective area increases more than that of sound area. During the cooling period, it acts again as insulator, but this time surface temperature of the defective area decreases more than that of sound area. In addition, the time that is necessary to reach a thermal balance between sound and defective areas creates a time-lag between the transition time to and from the heating period, and thus between the transition time to and from higher surface temperature at the defective area (Chew, 1998; Edis et al, 2015). In Figure 1, thermograms of a ceramic cladding facing south with delamination problem, as detected by hammer tapping control, are given to represent the aforementioned condition (Edis et al, 2014). At 10:00, when there was solar and convective heat gain, most areas with delamination were visible with a surface temperature increase. At 17:00, when there was still solar heat gain but exterior air temperature was dropping, areas with delamination were not visible. At 19:00, the wall was totally under shadow, and indications started to be visible at some but not all the defective areas with a decrease in surface temperature. The figure shows also the effect of inspection time on the performance of inspection method, and the importance of predicting thermal response to interpret thermograms.

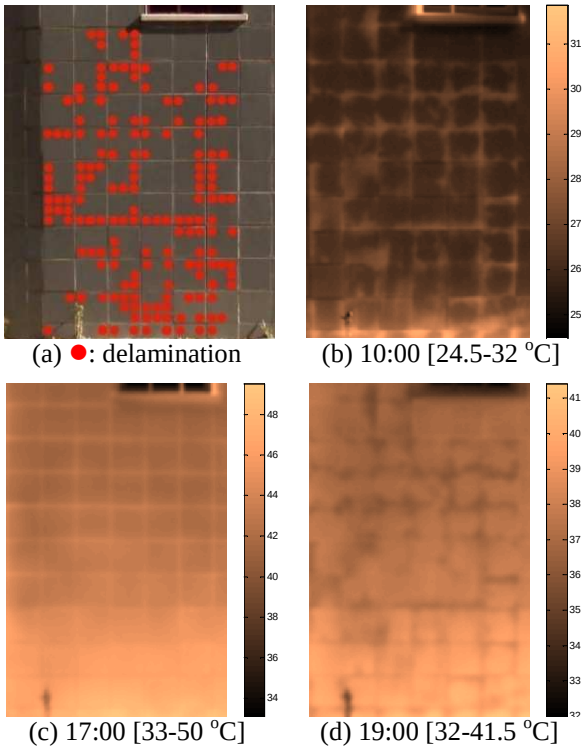

Figure 1 (a) Delamination map of a ceramic cladding, and (b-d) thermograms of it taken at different hours (Edis et al, 2014). Note: Values within square brackets show minimum and maximum temperatures observed.

PREDICTING THERMAL RESPONSE OF AN ETICS IN ISTANBUL (TURKEY) FOR DELAMINATION DETECTION BY IRT

Scope and objective

The most populated city of Turkey is Istanbul, where residential buildings constitute the largest share in all buildings, i.e. ca. 89% (SIS, 2000). Residential buildings in Istanbul usually have reinforced concrete structural frame with hollow clay brick infill walls. Use of ETICS with extruded polystyrene (XPS) is one of the common applications for thermally insulating these buildings.

In ETICS applications, delamination of the exterior render from the insulation and delamination of the insulation from the brick wall are two of the durability problems observed, not only in Turkey, but also in other countries (Daniotti et al, 2012). IRT can be used to detect these delaminations remotely, and proper maintenance measures can then be decided if necessary.

In the study, to assess the potential and performance of IRT using natural environmental conditions in detecting delamination present in an ETICS applied onto hollow clay brick infill wall, thermal simulations were performed considering the environmental conditions of Istanbul. Some supplementary simulations were also performed to evaluate the effects of the quality/precision of the brick model and interior environmental conditions on the results.

Computation process and variables

Numerical thermal simulations to compare the behaviour of sound and defective areas were performed by ANSYS 13 Fluent. The energy equation of the software to compute the heat flux in the solid regions is as follows (ANSYS, 2010):

$$\frac{\partial}{\partial t}(\rho h) + \nabla \cdot (\vec{v}\rho h) = \nabla \cdot (k\nabla T) + S_h \qquad (1)$$

In the wall model, three courses and three columns of hollowed clay brick were used. To understand the effect of the precision of the wall model on the results, a couple of simulations were performed on a wall model with solid bricks. In the remaining text, unless specified as studied on the model with solid bricks, all results given consider simulations performed on the model with hollowed bricks. Enclosed 1 cm thick air gap (i.e. delamination) was modelled at the centre of the model both horizontally and vertically, and its projected size on the surface was kept similar to that of the brick at the centre. Delamination of exterior render from thermal insulation ($_{rend}$) and delamination of thermal insulation from brick wall ($_{therm}$) were studied as separate cases. Transient three dimensional (3D) calculations were performed on grids with ca. 300.000 cells. Schematic section of the model and material characteristics used are given in Figure 2.

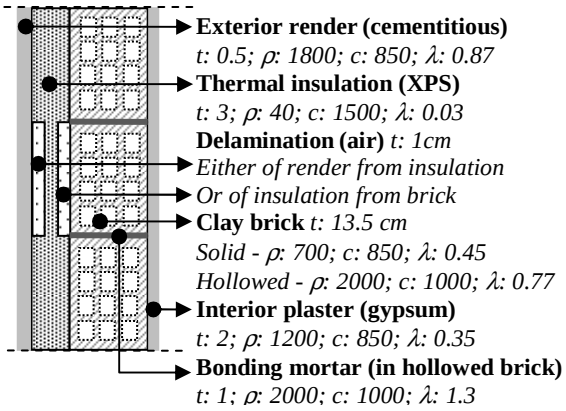

Figure 2 Section of the wall assembly studied and material characteristics used.

Hourly T_{ext} values of Istanbul were provided from Meteonorm 6 software. Simulations were performed for February 15th and July 21st, considering that minimum and maximum temperatures were given for these days in the annual dataset, respectively (Figure 3a). Air temperature was defined as 'free stream temperature (K)' under convective thermal boundary conditions using hourly transient profile for T_{ext} and constant 21^{o}C for T_{int}. Constant heat transfer coefficients of exterior and interior surfaces were defined as 25 and 8 W/m^{2}K respectively. To

understand the effect of T_{int} on the results, a couple of simulations with different T_{int} were also performed, and in the remaining text, it is specified whenever a T_{int} value other than 21 ^{o}C was used in the simulations.

The Fluent software computes solar effects usually in relation with transparent/translucent components. Therefore, solar load was applied onto the wall model by using an assumptive heat generating wall in front of the exterior side with a thickness of 0.001 m. Four cardinal directions, namely north (N), east (E), south (S), and west (W) were studied as different wall orientations. Solar radiation amount was determined by the 'Solar Calculator' of the Fluent software using the 'theoretical maximum' option. Depending on the direction of the wall, the hourly amount of generated heat (W/m^3) was determined using diffuse and/or ground reflected solar radiation on the vertical surface. The emissivity of a light-coloured render is ca. 0.90. The actual amount of solar load on the exterior surface decreased according to the emissivity value considering that general emissivity; i.e. wavelength independent emissivity and absorptivity of an object can be assumed to be the same as a corollary of Kirchoff's law. In Figure 3b, hourly amounts of heat applied on the exterior surface on February 15th and July 21st are given for walls facing different orientations. In the N facing walls, only the ground reflected solar radiation, and in the S facing walls, both ground reflected and diffuse radiation were considered. For the E and W facings walls, ground reflected radiation was considered during the hours when there was no solar exposure, and both types of solar radiation were considered during the hours of solar exposure.

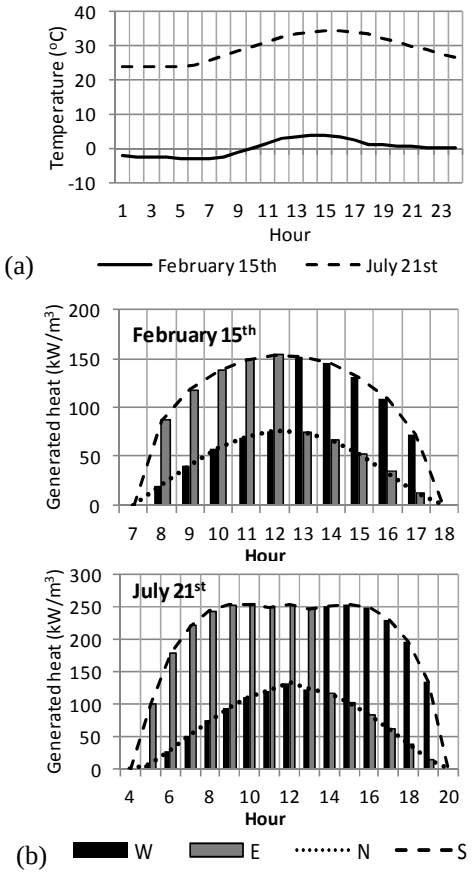

Figure 3 Hourly values of (a) T_{ext}, and (b) generated heat on the exterior wall surface as solar load.

Analysis procedure

Simulations were run for a 2-day period using the same hourly climate data, and results of the second day were used in the analysis to compensate the effect of initial thermal conditions on the results, if there was any. On the exterior surface, two monitoring points; one on the defective area and the other on the sound area were defined to record surface temperatures in each time step of 1-minute, and 15-minute averages of them were used in the further evaluations. In the analysis of the results, surface temperature difference between defective and sound areas (ΔT_{ed-es}) was used. In the cases where delamination of thermal insulation from the brick wall was studied, two other monitoring points were also defined on the interior surface to collect temperature data, and again, surface temperature difference between defective and sound areas (ΔT_{id-is}) was used in the analyses.

Simulation results

Analysis of $\Delta T_{ed-es\ (rend)}$ showed that (Figure 4):

- During solar exposure, $|\Delta T_{ed-es(rend)}|$ in July 21st was generally higher than that of in February 15th, while it was the opposite when there was no solar exposure, i.e. during night-time;
- In February 15th, $\Delta T_{ed-es\ (rend)}$ had generally stable behaviour ranging between 0.02 ^{o}C and -0.05 ^{o}C. However, in July 21st it had some downward and upward peaks at the beginning of solar exposure ranging between 0.17 ^{o}C and -0.20 ^{o}C;
- Change of orientation generally affected $\Delta T_{ed-es(rend)}$ observed at the beginning and/or at the end of (direct) solar exposure both in summer and winter conditions. The highest difference of 0.007 ^{o}C was observed between E and W at 13:00 in summer.

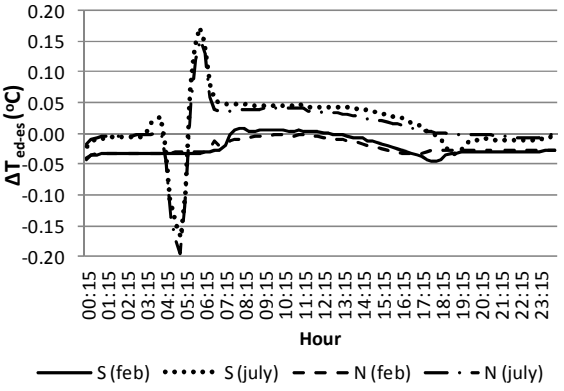

Figure 4 $\Delta T_{ed-es\ (rend)}$.

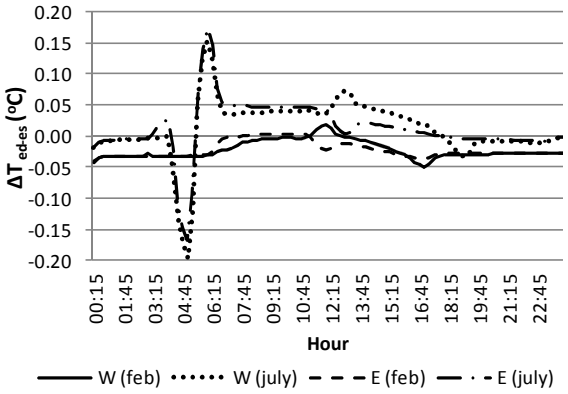

Figure 4 (Cont'd)

Analysis of $\Delta T_{ed\text{-}es(therm)}$ showed that (Figure 5):

- In summer conditions, surface temperature of the defective area was higher than that of sound area during daytime, while it was usually the other way around in winter conditions, where the solar load and T_{ext} was considerably lower than that of summer;
- During solar exposure, $|\Delta T_{ed\text{-}es(therm)}|$ in July 21st was generally higher than that of in February 15th, while it was the opposite when there was no solar exposure, i.e. during night-time;
- Change of orientation generally affected $\Delta T_{ed\text{-}es(term)}$ observed at the beginning and/or at the end of (direct) solar exposure in summer conditions, and the highest difference of 0.018 °C was observed between E and W facing walls between 13:30 and 14:15. It was similar in winter conditions as well, and the highest difference of 0.01 °C was observed between E and W facing walls at 12:30;
- In summer conditions, $\Delta T_{ed\text{-}es(therm)}$ was slightly lower than $\Delta T_{ed\text{-}es(rend)}$, when peaks occurring at the beginning of solar exposure were ignored. It was also low in winter conditions, but not as low as that of summer period.

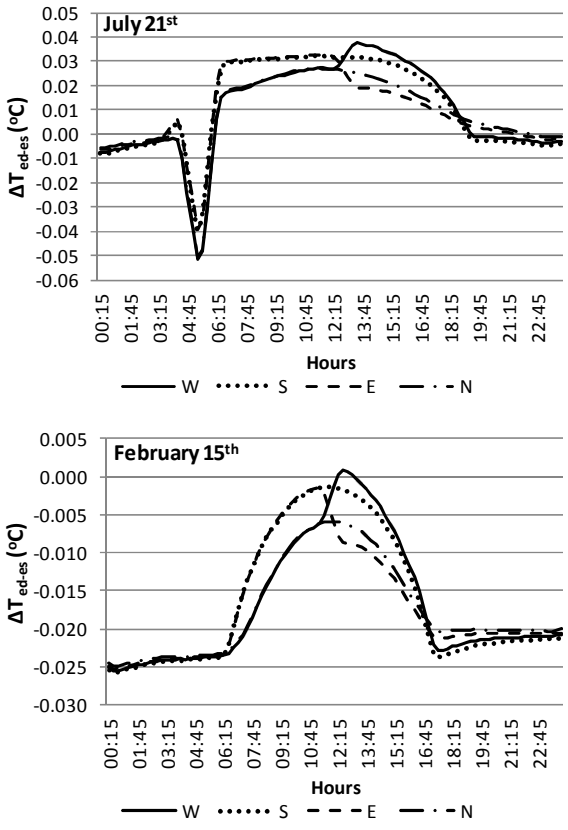

Figure 5 $\Delta T_{ed\text{-}es\ (therm)}$.

Analysis of $\Delta T_{id\text{-}is(therm)}$ showed that (Figure 6):

- $|\Delta T_{id\text{-}is(therm)}|$ was higher in summer condition than in winter condition, both with a sinusoidal action;
- Both in summer and winter conditions, $\Delta T_{id\text{-}is(therm)}$ was considerably lower than $\Delta T_{ed\text{-}es(therm)}$. In July 21st, for instance, $\Delta T_{id\text{-}is(therm)}$ ranged between 0.005 °C and -0.007 °C, while $\Delta T_{ed\text{-}es(therm)}$ ranged between 0.037 °C and -0.052 °C with an apparent effect of solar exposure on surface temperatures.

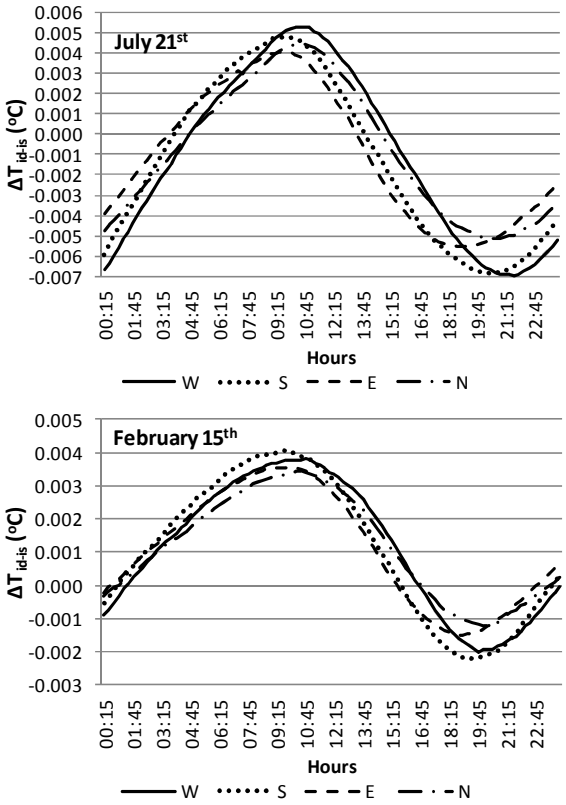

Figure 6 $\Delta T_{id\text{-}is\ (therm)}$.

Simulations to understand the effect of T_{int} on $\Delta T_{ed\text{-}es\ (rend)}$ were performed for S facing wall considering slightly higher values obtained in that direction. T_{int} was set to 18 °C and 24 °C in summer and winter conditions respectively. Analysis showed that (Figure 7);

- In summer during daytime, $\Delta T_{ed\text{-}es\ (rend)}$ was lower but more stable when T_{int} was decreased;

- In winter during night-time, $|\Delta T_{ed\text{-}es\ (rend)}|$ increased when T_{int} was increased.

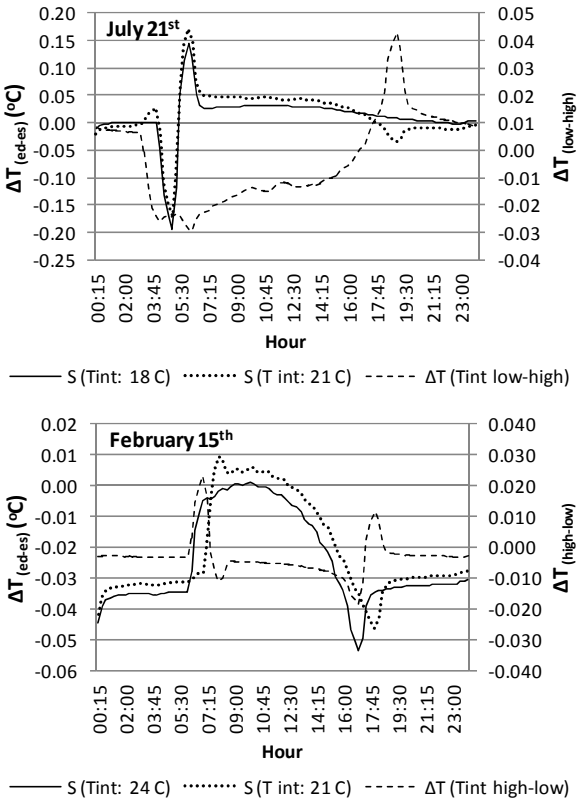

Figure 7 Change in $\Delta T_{ed\text{-}es\ (rend)}$ with the change in T_{int}.

Simulations using the model with solid bricks were performed for summer conditions for W and E facing walls with delamination of render from thermal insulation. Comparative analysis with the model using hollowed bricks showed that ΔTed-es(rend) had similar trend throughout the day, and the difference between ΔTed-es(rend) results of two models were small; i.e. maximum of 0.013 oC (Figure 8).

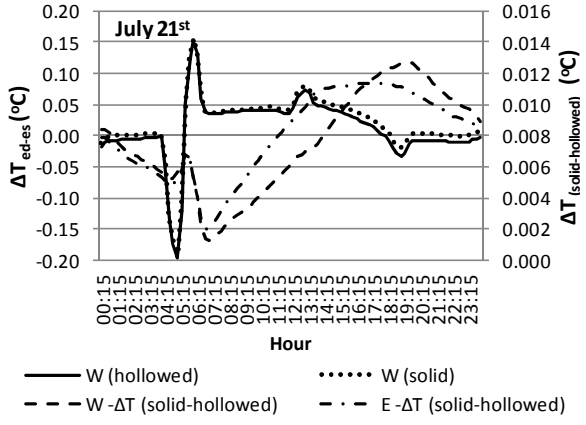

Figure 8 $\Delta T_{ed\text{-}es\ (rend)}$ results of wall models with solid and hollowed bricks, and difference between results.

DISCUSSION ON THE SIMULATION RESULTS AS A BACKUP FOR DELAMINATION DETECTION BY IRT IN ETICS APPLICATIONS

Simulations performed to predict the effect of delamination between ETICS layers on the evolution of surface temperatures showed as expected that, under dynamic thermal conditions, surface temperature of the defective area varied from that of sound area because of the air gap formed by the delamination. Researchers studied on delamination detection by IRT using natural environmental conditions to trigger surface temperature variations also reported similar behaviour; e.g. (de Freitas et al, 2014; Washer et al, 2010; Grinzato et al, 1998). In these studies, except the first one, they also reported that the magnitude of surface temperature variation changed in relation with the depth of delamination, which is in line with the simulation results presented in this paper. Therefore, it is found safe to assume that simulation results are valid in terms of general behaviour, although the magnitudes of surface temperature differences between sound and defective areas cannot be verified because of the differences in exposure conditions and assembly characteristics.

Simulations performed to understand the effect of delamination between ETICS layers on surface temperatures show that;

- $\Delta T_{ed\text{-}es(rend)}$ will be higher during daytime in summer conditions, when compared to that of during night-time or to that of winter conditions. It will also be stable in general during that period, except at the beginning or at the end of (direct) solar exposure. At the beginning of solar exposure, it is likely to have peaks ranging between 0.17 ^{o}C and -0.20 ^{o}C, and afterwards it will likely be stable at ca. 0.05 ^{o}C until noon;
- $\Delta T_{ed\text{-}es(therm)}$, although it won't be as high as $\Delta T_{ed\text{-}es(rend)}$, will be high during daytime in summer conditions, and during night-time in winter conditions. It is likely to be ca. 0.02-0.03 ^{o}C in the former, and ca. 0.02 ^{o}C in the latter;
- $\Delta T_{id\text{-}is(therm)}$ will be the lowest among the others both in summer and winter conditions. $|\Delta T_{id\text{-}is(therm)}|$ is likely to be not more than 0.01 ^{o}C.

Thermal sensitivity of infrared (IR) cameras is continuously improving, and currently it is possible to detect temperature differences as low as 0.04 ^{o}C with hand-held IR cameras. However, during *in situ* applications, factors such as reflection of surrounding objects or local variation of surface characteristics due to e.g. stains and efflorescence may also create surface temperature variations as low as that. Therefore, higher temperature differences are usually preferred to detect a defect precisely.

In terms of detecting delamination between ETICS layers by IRT using natural environmental

conditions, simulation results show that detection of delamination of thermal insulation from the brick wall cannot be possible, neither from the outside nor from the inside, in the studied environmental conditions, because of low $\Delta T_{ed\text{-}es(therm)}$ and $\Delta T_{id\text{-}is(therm)}$. On the other hand, in the case of delamination of render from thermal insulation, simulation results show that there is a good potential to detect delamination in summer conditions, especially when time-dependent IRT inspection is performed between sunrise and noontime. Peaks occurring at the beginning of solar exposure will help identifying the defect, although $\Delta T_{ed\text{-}es(rend)}$ will be low but stable afterwards. However, further *in situ* IRT inspections on actual delamination cases are also necessary to validate that.

Researchers working on developing/improving IRT methods use computer simulation to predict and/or verify IRT inspection results (e.g. (de Freitas et al, 2014; Edis et al, 2015)). It also allows determining proper inspection period and time in terms of exterior environmental conditions. In addition, as simulations of different T_{int} conditions show, it may help setting interior environmental conditions during IRT inspection to achieve higher surface temperature variations between sound and defective areas.

As in other fields of applications of computer simulation, in its use as backup for IRT applications, characteristics of the numerical model (e.g. precision in the geometrical characteristics of the assembly) is one of the factors affecting the accuracy of results. In terms of ease of use or user-friendliness of the simulation software, necessary modelling effort/time is important, but it is also in conflict with the precision of the numerical model, since over simplified models may cause errors in the results.

To understand the effect of using solid bricks in the wall model instead of hollowed ones for decreasing the modelling effort, a couple of simulations were performed on a wall model with solid bricks, and the change in the computation results was small, showing that there is a potential to use solid bricks in thermal simulations having similar objectives. However, further simulations and in deep analysis are necessary to verify it.

CONCLUDING REMARKS

In IRT applications, inspection time and conditions have important effects on detecting defects properly. In addition, some defects may not be detected by IRT since surface temperature difference occurring between sound and defective area is not sufficient. To determine proper inspection timing and to evaluate the potential of IRT in detecting defects, computer simulation can be used as a tool. In the paper, detection of delamination between ETICS layers by IRT is considered, and thermal simulations performed with similar objectives, as mentioned above, are presented.

Thermal simulations performed for ETICS applications in Istanbul (Turkey) showed that IRT using natural environmental conditions has good potential to detect delamination of exterior render from thermal insulation in summer conditions, but further *in situ* IRT inspections are necessary to verify simulation results and to determine its exact potential. Detection of delamination of thermal insulation from the brick wall by IRT seems to be not possible according to the simulation results. However, further *in situ* IRT inspections are also necessary to verify this finding.

NOMENCLATURE

ρ = Density (kg/m^3)
λ = Thermal conductivity (W/mK)
h = Sensible enthalpy (J/kg)
v = Velocity (m/s)
T = Temperature (◦C, K)
S_h = Volumetric heat source (W/m^3)
t = Thickness (cm)
c = Specific heat capacity (J/kg K)
ΔT = Temperature difference (◦C)
$_{es, ed}$ = Projection of sound and defective areas on the exterior surface respectively
$_{is, id}$ = Projection of sound and defective areas on the inteior surface respectively
$_{ext}$ = Exterior air
$_{int}$ = Interior air
$_{(rend)}$ = Delamination of render from thermal insulation
$_{(therm)}$ = Delamination of thermal insulation from brick

REFERENCES

ANSYS, 2010. ANSYS R13.0 - ANSYS FLUENT theory guide, ANSYS Inc., Canonsburg.

Chew, M.L. 1998. Assessing building facades using infra-red thermography, Structural Survey, 16(2), 81-86.

Daniotti, B., Re Cecconi, F., Paolini, R., Galliano, R., Ferrer, J., Battaglia, L. 2012. Durability evaluation of ETICS: analysis of failures case studies and heat and moisture transfer simulations to assess the frequency of critical events, 4th Portuguese Conference on Mortars and ETICS, Coimbra, Portugal. http://www.apfac.pt/congresso2012/comunicacoes/Paper%20104_2012.pdf. Access: 7.1.2015.

de Freitas, S.S., de Freitas, V.P., Barreira, E. 2014. Detection of façade plaster detachments using infrared thermography – A nondestructive technique. Construction and Building Materials, 70(1): 80-87.

Edis, E., Flores-Colen, I., De Brito, J. 2015. Building thermography: Detection of delamination of adhered ceramic claddings using the passive approach, Journal of Nondestructive Evaluation, 34:268.

Edis, E., Flores-Colen, I., De Brito, J. 2014. Time-dependent passive infrared thermographic inspection of facades, Proceedings of 13th International Conference on Durability of Building Materials and Components - XIII DBMC, São Paulo, Brazil, pp. 853-860.

Grinzato, E., Vavilov, V., Kauppinen, T., 1998. Quantitative infrared thermography in buildings. Energy and Buildings, 29(1): 1-9

ISO, 1983. ISO 6781 Thermal insulation – qualitative detection of thermal irregularities in building envelopes – infrared method, International Organization for Standardization, Switzerland.

Rosina E, Ludwig N. 1999. Optimal thermographic procedures for moisture analysis in building materials, Proceedings of society of photographic instrumentation engineers (SPIE), vol. 3827, p. 22-33.

Santos, C.P., Matias, L., Magalhães, A.C., Veiga, M.R. 2003. Application of thermography and ultra-sounds for wall anomalies diagnosis. A laboratory research study, Proceedings of the International Symposium-Non-Destructive Testing in Civil Engineering, Berlin. http://www.ndt.net/article/ndtce03/papers/v082/v082.htm, Accessed: November 2013.

SIS, 2000. Building Census 2000, State Institute of Statistics (SIS) – Prime Ministry of Republic of Turkey, Ankara.

Washer, G., Fenwick, R., Bolleni, N., 2010. Effects of Solar Loading on Infrared Imaging of Subsurface Features in Concrete. Journal of Bridge Engineering, Vol. 15, Special Issue: Bridge Inspection and Evaluation, 384-390.